

doi:10.15199/48.2019.05.15

The use of elastic net and neural networks in industrial process tomography

Abstract. The article presents an innovative approach based on electrical capacitance tomography (ECT) improving industrial tomography processes. Thanks to the application of elastic net and artificial neural networks, algorithms have been developed that enable obtaining high quality images and resolutions. During the experiments, two methods of reconstructing "pixel by pixel" images were compared. Both methods showed high efficiency, and the use of elastic net accelerated the operation of the ECT system.

Streszczenie. W artykule przedstawiono nowatorskie podejście oparte na ECT usprawniające procesy tomografii przemysłowej. Dzięki zastosowaniu elastic net i sztucznych sieci neuronowych opracowano algorytmy umożliwiające uzyskanie obrazów o wysokiej jakości i rozdzielczości. W trakcie przeprowadzonych eksperymentów porównano dwie metody rekonstrukcji obrazów "pixel by pixel". Obie metody wykazały się wysoką skutecznością, a wykorzystanie elastic net przyspieszyło działanie systemu ECT. (Zastosowanie elastic net i sieci neuronowych w tomografii przemysłowej).

Keywords: industrial process tomography, neural networks, elastic net, electrical tomography.

Słowa kluczowe: przemysłowa tomografia procesowa, sieci neuronowe, elastic net, tomografia elektryczna.

Introduction

Industrial Process Tomography (IPT) is a non-invasive and non-destructive imaging [1] technique used in various industries for processes in which knowledge about the interior of the object is required [2], [3]. A common reason for using IPT is that it plays an important role in the continuous monitoring of systems, allowing better understanding and ensuring the quality of industrial processes. IPT provides fast and dynamic response, facilitates process control, including on-line, enables error detection and system failures in real time [4]. In addition, thanks to IPT, the process characteristics can be quantified, with data included in the overall process control strategy. Finally, IPT provides robust experimental means to optimize the design and operation of a process tank or pipeline by developing a model and validation.

Industrial process tomography (IPT) applications are usually a challenge for obtaining spatial data from observation beyond the boundaries of the process. The wireless sensor network technology with their return loops will be the basis for production control. The decisive difference in mass production of chemicals, metals, building materials, food and other goods is that common process sensors provide only local measurements such as temperature, pressure, fill level, flow rate or species concentration. However, in most production systems, such local measurements are not representative of the overall process and therefore spatial solutions are needed. Here the future belongs to the dispersed and imaging sensors.

The tomograph can be adapted to the requirements of a

given company and to the specifics of a given industry. The prepared solution can effectively support the quality of products in automated production lines by identifying shapes, detecting cracks and damage, and presenting three-dimensional visualization of industrial processes. This is especially important for dairy producers, where the foaming substance can lead to production losses, or beer, where the foams are produced as a natural part of the brewing process. In turn, in the mining industry, control of the foam layer in the flotation chamber is a critical parameter of the process. In addition, all these elements have a direct impact on the overall profitability of production by improving the specification of the final product and processing efficiency.

Advanced automation and process control play a key role in maintaining competitiveness. While costly technological devices and production lines can be regarded as the heart of industrial production, control systems and information technologies are the brain. They provide the flexibility to quickly adapt production processes to changing customer requirements and ensure safety and efficiency at the lowest possible cost of resources and energy. Complex system to the data acquisition, the image reconstruction with cloud computing model were shown in Fig. 1. IPT systems are usually based on electrical capacitance tomography (ECT) [5]–[7].

Due to its implementation nature, process tomography can use a lot of different methods and techniques, including: resistive tomography (EIT) [8], [9], magnetoacoustics [10], multipath tomography [11], artificial

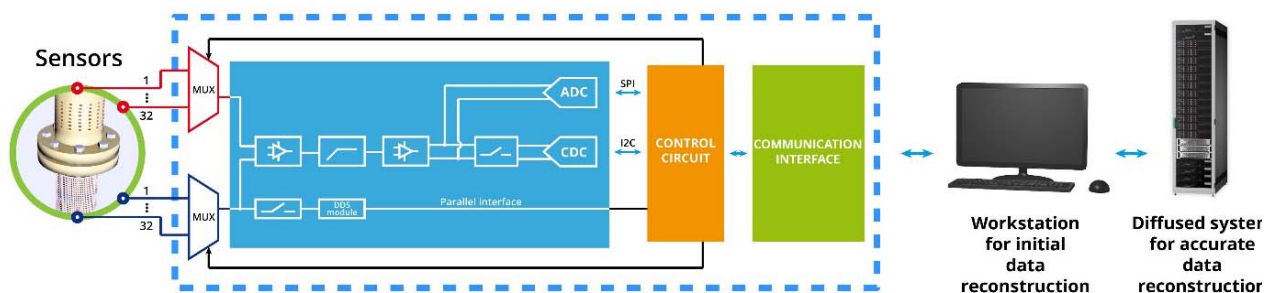


Fig.1 Schematic model of Smart ECT measurement system

intelligence [12], linear programming [13], machine learning [14] etc.

Multiphase flows and multiphase reactors are commonly found in the energy industry in coal gasification (carbon dioxide emission process), combustion chambers, refineries, oil drilling and pipeline transport [15,16]. The naturally complex nature of multiphase flows requires a multidimensional measurement technique that provides real time monitoring of process dynamics and physical flow properties. The use of capacitive sensors enables the visualization of coal combustion processes, fuel, emission control and optimization of energy generation.

In IPT the visualization of the inside of the investigated body is obtained on the basis of the recorded capacitance measurements. In this paper hardware issues, measurements and the image reconstruction are described but the main focus is on the processing of electrical data.

Materials and methods

The aim of the research was to develop an efficient method of data processing in the ECT type process tomograph. For this purpose, a reactor model was constructed under laboratory conditions, as shown in Fig. 2.



Fig.2. The physical model of the reactor

The physical model of the reactor was equipped with 64 electrodes. In the presented research, 16 electrodes were connected, which generate one measurement vector containing 96 electrical capacitance values.

Fig. 3 shows a schematic of an algorithm for converting electrical data into a reconstructed image.

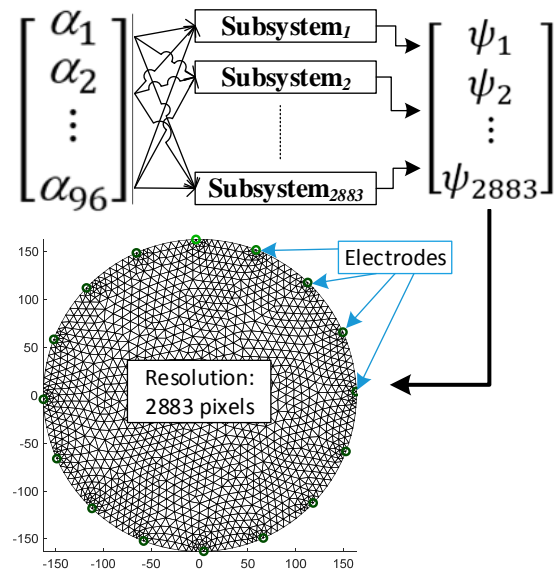


Fig.3. Model of the ECT system converting electrical signals into 2D image of cross-section

The cross-section of the tested reactor was divided into a mesh with 2883 pixels, which consist in the resolution of the output image. The color of each individual pixel is determined separately based on the real number generated by the separately trained subsystem. This means that the number of subsystems in the considered case is 2883. Each subsystem is fed by the same input vector of 96 predictors values. In order to accelerate the operation of the IPT system, as well as to immunize the tomographic system to noise the input data, the elastic net technique was used, thanks to which the number of input data was reduced [17].

As part of the research, two drivers for ECT processing were developed. The first of them functioned according to the workflow presented in Fig. 4. The workflow of the second controller, without elastic net, is shown in Fig.5. Fig. 4 shows a hybrid subsystem workflow for pixel ψ_{2000} that reduces the input vector from 96 to 26 values. Then a neural network based on 26 values generates a real number, based on which one of the 2883 pixels of the reconstructed image is displayed. Fig. 5 shows an analogous workflow, however, without the reduction of the predictors vector. In this case, ANN processes all 96 input data into one real number.

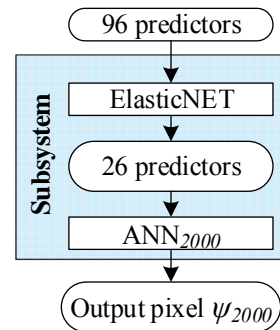


Fig.4. Model of elastic net + ANN hybrid subsystem dedicated to a single pixel ψ_{2000}

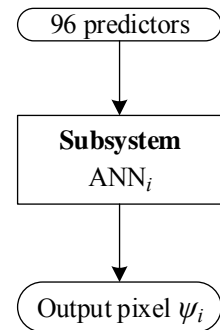


Fig.5. Model of pure ANN subsystem dedicated to a single pixel ψ_i

Elastic net is a regularized regression method that linearly combines the L1 and L2 penalties of the Least Absolute Shrinkage and Selection Operator (Lasso) and ridge methods [18]. Lasso is a regularization technique. It can be used to reduce the number of predictors in a regression model or select among redundant predictors. For a given value of λ , a nonnegative parameter, Lasso solves the problem (1):

$$(1) \quad \min_{\beta_0, \beta} \left(\frac{1}{2N} \sum_{i=1}^N (y_i - \beta_0 - x_i^T \beta)^2 + \lambda \sum_{j=1}^p |\beta_j| \right)$$

where: N - the number of observations; y_i - the response at observation i ; x_i - data, a vector of p values at observation i ; λ - a positive regularization parameter corresponding to one value of Λ .

The parameters β_0 and β are scalar and p -vector respectively. For an α strictly between 0 and 1, and a positive λ , elastic net solves the regularization problem (2):

$$(2) \quad \min_{\beta_0, \beta} \left(\frac{1}{2N} \sum_{i=1}^N (y_i - \beta_0 - x_i^T \beta)^2 + \lambda P_\alpha(\beta) \right)$$

where

$$P_\alpha(\beta) = \frac{(1-\alpha)}{2} \|\beta\|_2^2 + \alpha \|\beta\|_1 = \sum_{j=1}^p \left(\frac{(1-\alpha)}{2} \beta_j^2 + \alpha |\beta_j| \right)$$

When $\alpha = 1$ elastic net is the same as Lasso. As α decreases toward 0, elastic net approaches ridge regression. For other values of α , the penalty term $P_\alpha(\beta)$ interpolates between the L1 norm of β and the squared L2 norm of β .

Fig. 6 shows a Cross-Validated MSE (mean squared error) of elastic net with $\alpha = 0.2$. The figure shows two specific Lambda values with green and blue dashed lines. The green, dashed line indicates the value of Lambda with a minimum cross-validated mean squared error (LambdaMinMSE). The blue, dashed line indicates the greatest Lambda that is within one standard error of the minimum MSE (Lambda1SE). This Lambda value makes the sparsest model with relatively low MSE.

Fig. 7 shows the x-axis from the L1 norm of the coefficients in B. The x-axis at the top of the list of the values of freedom (df), meaning the number of nonzero coefficients of B. B represents the coefficients of a sequence of regression fits, as returned from the lasso functions.

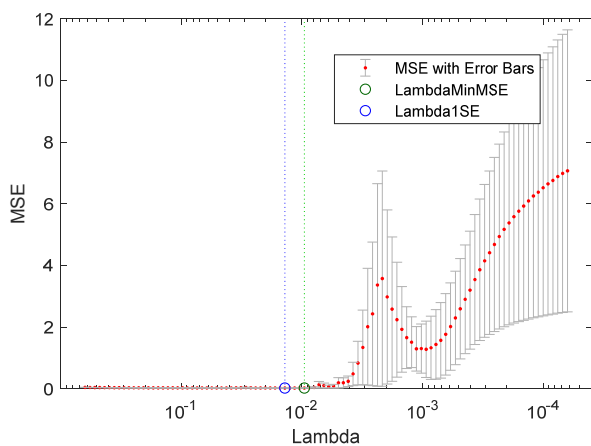


Fig.6 Cross-Validated MSE of elastic net fit Alpha = 0.2

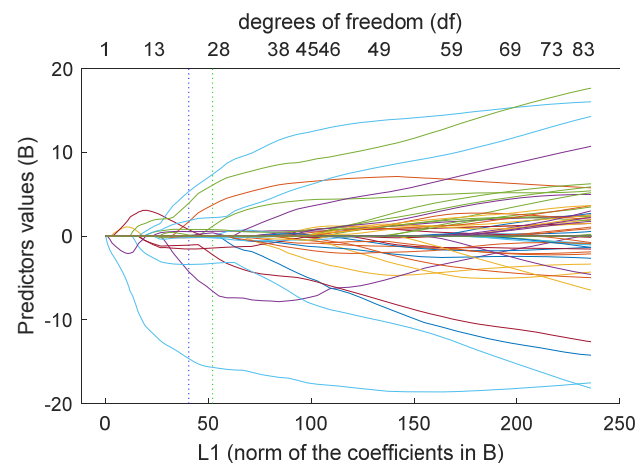


Fig.7 Trace plot of coefficients B vs. L1 Fit by elastic net (Alpha = 0.2)

By analysing Fig. 6 and Fig. 7, we can conclude that the regularization process performed by the elastic net method works properly. With Alfa = 0.2, the algorithm optimally selects Lambda coefficients by implementing the MSE minimization criterion. In Fig. 7, each line defines the course of the L1 norm for each of the 96 predictors during the elastic net regularization process.

After reducing the predictors' vector, a system of 2833 neural networks was trained. All neural networks had a structure A_n-10-1 while the original shape of the subsystem was as follows: $96-ElasticNet-A_n-10-1$. Each of the 2883 pixels of the image has its own subsystem, which at the

beginning is fed by a vector of 96 electrical values. After reducing the number of predictors by the elastic net method, there are A_n predictors that feed the neural network. ANN has one hidden layer with 10 neurons and one neuron in the output layer. Various neural network configurations were tested during the study, but it was found that excessive increase in the number of neurons in the hidden layer does not improve the quality of the network.

Table 1 presents the learning results of the ANN network for pixel ψ_{2000} , after prior reduction of the predictors using the elastic net method. The data set numbered 50,000 cases. The entire dataset was divided into 3 parts in 70/15/15 proportions. In this way, the following sets were created: training, validation and testing set. The network learning process was carried out using the Levenberg-Marquardt algorithm. The highest MSE value was obtained for the test set, which is a normal situation. It is important that the MSE value is low, close to zero, and is around 0.0089. In turn, the regression is high and is at the level of 0.896, which also indicates good quality of the obtained neural network. Analyzing all the obtained values of MSE and R, it can be concluded that the network has not been learned and has generalization capabilities.

Table 1. Training results of ANN₂₀₀₀ for pixel ψ_{2000}

	Samples	MSE	R
Training:	35000	7.35353e-3	9.11097e-1
Validation:	7500	8.22964e-3	8.93213e-1
Testing:	7500	8.97455e-3	8.95855e-1

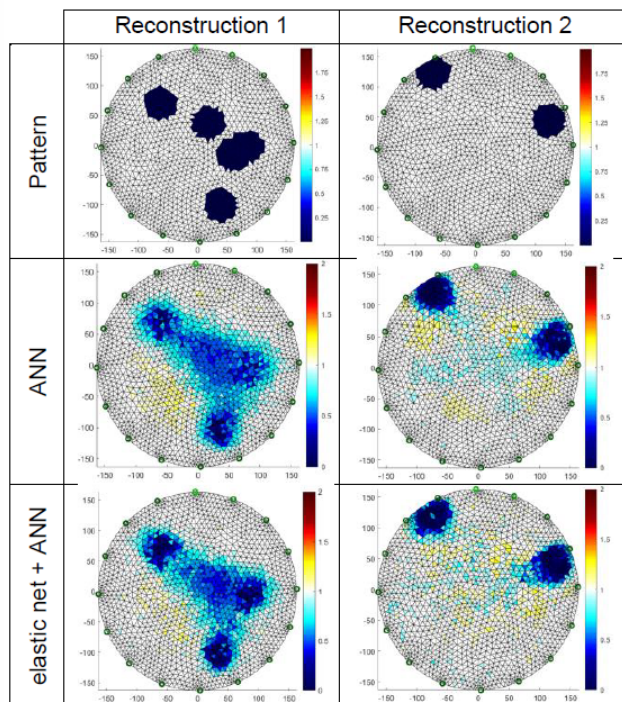


Fig.8 Comparison of reconstructions performed with ANN and (elastic net + ANN) methods

Results

Fig. 8 presents a comparison of the final reconstructions performed with two methods: ANN and the hybrid method (elastic net + ANN). Comparing the reconstructed images with the patterns, one can notice the high accuracy of the mapping both in the position of the anomaly as well as the

number of objects. It can be noticed that also the conductance values of the reconstructed objects hidden inside the reactor are close to their pattern values.

An important observation is that the reconstructions made with both methods are very similar to each other. This means that the reduction of input variables by the elastic net method did not reduce the quality of the ECT system. At the same time, the reduction of the number of predictors significantly accelerated the speed of the system's operation. An even greater advantage of reducing the predictors was obtained at the stage of neural network training. Because there is a need to learn 2883 separate ANNs in the system under study, the learning time has been reduced from 24 hours (pure ANN) to 3 hours (elastic net + ANN).

Conclusions

The article presents research on an innovative approach to Industrial Process Tomography based on ECT. Using artificial neural networks, an algorithm for converting input electrical data into an image was developed. Each individual neural network implements a regression problem, generating one real number defining the colour of one pixel of the reconstructed image. In this way, the image presented on the mesh with a resolution of 2883 pixels requires the training of 2883 neural networks. During the tests, the method of reducing the number of input variables by removing redundant predictors and those that have little influence on the output value was investigated. It turned out that, despite the reduction of independent variables, the image quality is comparable to that reconstructed using the ANN method with a full input vector (96 values). The reduction of the predictors enabled the ECT system to be accelerated twice. In addition, the training time of many ANNs has shortened from 24 to 3h.

A very important advantage of systems subjected to the reduction of independent variables is the increase of their resistance to various types of data noise. Observing the differences between ANN and (elastic net + ANN) images in the case of Reconstruction 1 (Fig. 8), it can be seen that (elastic net + ANN) better reflects the reference image rather than pure ANN. Although it may initially be a surprise, it turns out that this effect may be the result of better effectiveness in the case of data in which noise and interference occur. Summing up, as a result of conducted laboratory and simulation experiments, it was found that the use of hybrid systems such as elastic net + ANN gives good results.

Authors: Tomasz Rymarczyk, Ph.D. Eng., University of Economics and Innovation, Projektowa 4 & Netrix S.A., Lublin, Poland, e-mail: tomasz&Rymarczyk.com; Grzegorz Kłosowski, Ph.D. Eng., Lublin University of Technology, Nadbystrzycka 38A, Lublin, Poland, E-mail: g.klosowski@pollub.pl.

REFERENCES

- [1]. Lopato, P., Chady, T., Sikora, R., Gratkowski, S. & Ziolkowski, M. Full wave numerical modelling of terahertz systems for nondestructive evaluation of dielectric structures. *COMPEL-The international journal for computation and mathematics in electrical and electronic engineering*. 32 (2013), 736–749
- [2]. Garbaa, H., Jackowska-Strumiłło, L., Grudzień, K. & Romanowski, A. Application of electrical capacitance tomography and artificial neural networks to rapid estimation of cylindrical shape parameters of industrial flow structure. *Archives of Electrical Engineering*. 65 (2016), 657–669
- [3]. Rymarczyk, T., Kłosowski, G. & Kozłowski, E. A Non-Destructive System Based on Electrical Tomography and Machine Learning to Analyze the Moisture of Buildings. *Sensors*, (18) 2018, 2285
- [4]. Dusek, J., Hladky, D. & Mikulka, J. Electrical impedance tomography methods and algorithms processed with a GPU. in 2017 Progress In Electromagnetics Research Symposium - Spring (PIERS), (2017), 1710–1714
- [5]. Kryszyn, J. & Smolik, W. Toolbox for 3d modelling and image reconstruction in electrical capacitance tomography. *Informatyka, Automatyka, Pomiar w Gospodarce i Ochronie Środowiska (IAPGOŚ)*, 7 (2017), np.1, 137-145
- [6]. Kryszyn, J., Wanta, D. M. & Smolik, W. T. Gain Adjustment for Signal-to-Noise Ratio Improvement in Electrical Capacitance Tomography System EVT4. *IEEE Sensors Journal*, 17 (2017), 8107–8116
- [7]. Grudzien, K., Chaniecki, Z., Romanowski, A., Sankowski, D., Nowakowski, J., & Niedostatkiwicz, M. Application of twin-plane ECT sensor for identification of the internal imperfections inside concrete beams. *Instrumentation and Measurement Technology Conference Proceedings (I2MTC)*, 2016 IEEE International. IEEE, (2016), 7520512
- [8]. Filipowicz, S. F. & Rymarczyk, T. Measurement Methods and Image Reconstruction in Electrical Impedance Tomography. *Przegląd Elektrotechniczny* 88 (2012), no. 6, 247–250
- [9]. Rymarczyk, T. & Kłosowski, G. Application of neural reconstruction of tomographic images in the problem of reliability of flood protection facilities. *Eksploatacja i Niezawodność – Maintenance and Reliability*, 20 (2018), no. 3, 425–434
- [10]. Ziolkowski, M., Gratkowski, S. & Zywicka, A. R. Analytical and numerical models of the magnetoacoustic tomography with magnetic induction. *COMPEL-The international journal for computation and mathematics in electrical and electronic engineering*. 37 (2018), no.2, 538–548
- [11]. Polakowski, K., Filipowicz, S. F., Sikora, J. & Rymarczyk, T. Quality of imaging in multipath tomography. *Przegląd Elektrotechniczny* 85 (2009), no. 12, 134–136
- [12]. Mazurkiewicz, D. Maintenance of belt conveyors using an expert system based on fuzzy logic. *Archives of Civil and Mechanical Engineering*. 15 (2015), no. 2, 412–418
- [13]. Kłosowski, G., Kozłowski, E. & Gola, A. Integer Linear Programming in Optimization of Waste After Cutting in the Furniture Manufacturing. *International Conference on Intelligent Systems in Production Engineering and Maintenance* 637, (2018).
- [14]. Psuj, G. Multi-Sensor Data Integration Using Deep Learning for Characterization of Defects in Steel Elements. *Sensors*, 18 (2018), 292
- [15]. Wajman, R., Fiderek, P., Fidos, H., Jaworski, T., Nowakowski, J., Sankowski, D., & Banasiak, R. Metrological evaluation of a 3D electrical capacitance tomography measurement system for two-phase flow fraction determination. *Measurement Science and Technology*, 24 (2013), no. 6, 065302
- [16]. Rymarczyk T., Sikora J. Applying industrial tomography to control and optimization flow systems, *Open Physics*, 16 (2018), 332–345
- [17]. Zou, H. & Hastie, T. Regularization and variable selection via the elastic net. *Journal of the Royal Statistical Society: Series B (Statistical Methodology)*. 67 (2005), 301–320
- [18]. Alhamzawi, R. & Ali, H. T. M. The Bayesian adaptive lasso regression. *Mathematical Biosciences*. (2018).